ADP-Binding Site of *Escherichia coli* Succinyl-CoA Synthetase Revealed by X-ray Crystallography[†,‡]

Michael A. Joyce,[§] Marie E. Fraser,[§,||] Michael N. G. James,[§,||] William A. Bridger,[⊥] and William T. Wolodko*[,§]

Department of Biochemistry, University of Alberta, Edmonton, Alberta, Canada T6G 2H7, Medical Research Council of Canada Group in Protein Structure and Function, University of Alberta, Edmonton, Alberta, Canada T6G 2H7, and Office of the VP Research, University of Western Ontario, London, Ontario, Canada N6A 5B8

Received July 22, 1999; Revised Manuscript Received October 25, 1999

ABSTRACT: Succinyl-CoA synthetase (SCS) catalyzes the following reversible reaction via a phosphorylated histidine intermediate (His 246α): succinyl-CoA + P_i + NDP ↔ succinate + CoA + NTP (N denotes adenosine or guanosine). To determine the structure of the enzyme with nucleotide bound, crystals of phosphorylated *Escherichia coli* SCS were soaked in successive experiments adopting progressive strategies. In the first experiment, 1 mM ADP (>15 × K_d) was added; Mg^{2+} ions were omitted to preclude the formation of an insoluble precipitate with the phosphate and ammonium ions. X-ray crystallography revealed that the enzyme was dephosphorylated, but the nucleotide did not remain bound to the enzyme ($R_{working}$ = 17.2%, R_{free} = 22.8% for data to 2.9 Å resolution). Catalysis requires Mg^{2+} ions; hence, the "true" nucleotide substrate is probably an ADP−Mg^{2+} complex. In the successful experiment, the phosphate buffer was exchanged with MOPS, the concentration of sulfate ions was lowered, and the concentrations of ADP and Mg^{2+} ions were increased to 10.5 and 50 mM, respectively. X-ray diffraction data revealed an ADP−Mg^{2+} complex bound in the ATP-grasp fold of the N-terminal domain of each β-subunit ($R_{working}$ = 19.1%, R_{free} = 24.7% for data to 3.3 Å resolution). We describe the specific interactions of the nucleotide−Mg^{2+} complex with SCS, compare these results with those for other proteins containing the ATP-grasp fold, and present a hypothetical model of the histidine-containing loop in the "down" position where it can interact with the nucleotide ∼35 Å from where His 246α is seen in both phosphorylated and dephosphorylated SCS.

Succinyl-CoA synthetase (SCS)[1] catalyzes the reversible interchange of purine nucleoside diphosphate, succinyl-CoA, and P_i with purine nucleoside triphosphate, succinate, and CoA via a phosphorylated histidine intermediate (reviewed in refs *1* and *2*). As with other enzymes that bind nucleotides, Mg^{2+} ions are required, and the "true" substrate is probably a nucleotide−Mg^{2+} complex. Universally, SCS consists of two subunit types designated α and β; the catalytic unit carrying out the interchange is an αβ-dimer. This is true even for SCS from *Escherichia coli*, a heterotetramer, which has been shown to consist of two αβ-dimers that are catalytically independent (*3*). In the crystal structure of *E. coli* SCS, the α-subunit is seen to bind one of the substrates, CoA, and has a loop that includes the histidine residue (H246α) phosphorylated during catalysis (*4*). On the basis of the sequences of different β-subunits from isoforms of SCS in pigeon, Johnson et al. (*5*) proposed that the β-subunit confers the nucleotide specificity, implying that the β-subunit binds the nucleotide. Consistent with this implication, evidence from the recognition of a new structural motif (*6*), from the comparison of SCS with other enzymes possessing this motif (*7*), and from the results of studies using a photoactivated ATP analogue and site-directed mutagenesis (*8*) delimited the nucleotide binding site to an ATP-grasp fold in the β-subunit. The CoA-binding site and the proposed nucleotide binding ATP-grasp fold are located approximately 35 Å apart in SCS, and have been designated site I and site II, respectively (*8*). Catalysis of the full reaction would necessitate the movement of His 246α between these two sites,

[†] This work was funded by grants from the Medical Research Council of Canada (MRC Grants MT-2805 and GR-13303). M.A.J. was supported by a studentship from the Alberta Heritage Foundation for Medical Research.

[‡] The coordinates and the data have been submitted to the Research Collaboratory for Structural Bioinformatics (RCSB) Protein Data Bank (PDB). The PDB codes are 1CQI for the crystal structure of the complex of ADP and Mg^{2+} ions with dephosphorylated *E. coli* succinyl-CoA synthetase and 1CQJ for the crystal structure of dephosphorylated *E. coli* succinyl-CoA synthetase.

* To whom correspondence should be addressed. Telephone: (780) 492-2419. Fax: (780) 492-0886. E-mail: wtwt@obi-wab.biochem.ualberta.ca.

[§] Department of Biochemistry, University of Alberta.

[||] Medical Research Council of Canada Group in Protein Structure and Function, University of Alberta.

[⊥] University of Western Ontario.

[1] Abbreviations: SCS, succinyl-CoA synthetase; NDP, adenosine or guanosine 5′-diphosphate; NTP, adenosine or guanosine 5′-triphosphate; AMPPCP, β,γ-methyleneadenosine 5′-triphosphate; P_i, inorganic phosphate; CoA, coenzyme A; MOPS, 3-(*N*-morpholino)propanesulfonic acid; K_d, dissociation constant; *k*, scale factor for minimizing the difference between data sets; $|F_{o(native)}|$, structure factor amplitude observed for the native crystal; $|F_{o(soak)}|$, structure factor amplitude observed for the crystal after soaking; I_i, individual measurement of an intensity; *I*, observed intensity averaged from all equivalent reflections; $|F_o|$, observed structure factor amplitude; $|F_c|$, calculated structure factor amplitude; rms, root-mean-square; DD-ligase, D-Ala:D-Ala ligase; σ, standard deviation. Specific amino acid residues in given subunits of SCS are designated by the one- or three-letter code followed by the residue number and either α or β to indicate the subunit.

10.1021/bi991696f CCC: $19.00
Published on Web 12/09/1999

thus explaining why, in part, the formation of an active catalytic unit requires both α- and β-subunits.

Here we report the X-ray crystallographic results of soaking crystals of *E. coli* SCS with high concentrations of ADP and Mg^{2+} ions, proving that the ADP−Mg^{2+} complex binds in the ATP-grasp fold of the N-terminal domain of the β-subunit. We describe in some detail, to the limit of the resolution, the specific interactions of the nucleotide−Mg^{2+} complex with SCS, compare these results with those for other proteins that contain the ATP-grasp fold, and present a hypothetical model of the histidine-containing loop in the "down" position where it can interact with the nucleotide in site II.

EXPERIMENTAL PROCEDURES

Protein Purification and Crystallization. SCS was overexpressed in *E. coli* strain JM103 transformed with the expression plasmid pGS202 (*4*) and purified as previously described (*9*). Crystals of phosphorylated SCS were grown by microdialysis from precipitant solutions consisting of 1.93 M ammonium sulfate, 50 mM potassium phosphate, and 0.5 mM CoA (pH 7.3) (*10*).

Soaking of ADP into Crystals of SCS. Several experiments were carried out, with the design of successive trials based on the results of the preceding ones, before we were able to obtain a complex of nucleotide with the enzyme in the crystals.

In the first experiment, the membrane surrounding the dialysis button was cut away to allow excess protein to diffuse away from the crystals. After 4.5 h, the open buttons were transferred to freshly prepared precipitant solutions containing 1 mM ADP [$>15 \times K_d$ (*11*)]. Magnesium ions were not added since they would have formed an insoluble precipitate with the phosphate and ammonium ions. The crystals were left to soak for 48 h at room temperature prior to data collection.

The successful experiment was inspired by the work of Ray et al. (*12*), who presented stratagems for lowering the salt concentration prior to conducting a substrate soak. The dialysis buttons were transferred to a solution containing 1.85 M ammonium sulfate in 50 mM MOPS (pH 7.3) to lower the concentrations of the sulfate and phosphate ions. After approximately 24 h, the buttons were transferred to a solution containing 1.85 M ammonium sulfate, 50 mM MOPS, 5 mM $MgCl_2$, and 0.53 mM ADP (pH 7.2). The crystals were allowed to soak for an additional 24 h before the buttons were transferred to a solution containing 1.8 M ammonium sulfate, 50 mM MOPS, 10 mM $MgCl_2$, and 4.7 mM ADP (pH 7.2). After 20 h, the membrane was removed, and the buttons were transferred to the final soaking solution containing 1.8 M ammonium sulfate, 50 mM MOPS, 50 mM $MgCl_2$, and 10.5 mM ADP (pH 7.2) for 5 h prior to mounting the crystals for data collection.

Data Collection, Processing, and Refinement. The data were collected on beamline 6A2 at the Photon Factory in Japan using 1.0 Å X-rays with the screenless Weissenberg camera at approximately 10 °C (*13*). The methods for data collection and processing have been described previously (*4*). The statistics for two data sets, the first experiment and the successful experiment, are presented in Table 1.

Table 1: Statistics for the Two Data Sets

	first experiment	successful experiment
space group	$P4_322$	$P4_322$
no. of molecules per asymmetric unit	2	2
no. of crystals	6	6
resolution (Å)	2.9	3.3
no. of observations	258739	195264
at high resolution (range)	19746 (3.02−2.89 Å)	15389 (3.54−3.33 Å)
no. of unique reflections	45002	31753
at high resolution (range)	6283 (3.08−2.90 Å)	4445 (3.51−3.30 Å)
data completeness (%)	98.7	99.0
at high resolution (range)	96.9 (3.08−2.90 Å)	98.4 (3.51−3.30 Å)
R_{merge}[a] (%)	9.2	16.4
at high resolution (range)	35.0 (3.02−2.89 Å)	37.8 (3.54−3.33 Å)

[a] $R_{merge} = (\Sigma\Sigma|I_i - I|)/\Sigma\Sigma I$, where I_i is the intensity of an individual measurement of a reflection and I is the mean value for all equivalent measurements of this reflection.

Each data set was scaled to the high-resolution data set for native SCS (*7*), and SIGMAA-weighted electron density maps (*14*) were calculated using programs from the BIOMOL package (Gröningen, Holland). The program TOM (ALBERTA/CALTECH version 3.0) (*15*) was used to view the electron density maps and to build the molecular models into the electron density peaks. The atomic coordinates and *B*-factors were refined using the CNS suite of programs with standard protocols (*16*−*22*) over several rounds. Both torsion angle simulated annealing refinement and conjugate gradient minimization refinement were performed with maximum likelihood targets. Noncrystallographic symmetry restraints were applied to all atoms except those of residues at the crystal contacts. The programs PROCHECK (*23*) and WHATCHECK (*24*) were used to judge the stereochemistry and the weights for the restraints. WHATCHECK was also used to improve the unit cell dimensions. Changes in R_{free} were used to judge the refinement protocol. For the 3.3 Å data, no water molecules were included in the final model and only two *B*-factors were used for each residue, one for the main chain atoms and one for the side chain atoms.

RESULTS

The differences from the native data [$R_{diff} = 100\% \times \Sigma||F_{o(native)}| - k|F_{o(soak)}||/\Sigma|F_{o(native)}|$] were 10.8 and 23.6% for the data from the first and successful experiments, respectively. Initial difference maps in the first experiment showed clearly that the active site histidine residue was dephosphorylated, and that there was electron density for a phosphate (or sulfate) ion bound nearby in site I (Figure 1A). In the successful experiment, in addition to the dephosphorylated enzyme, there was electron density for the nucleotide and a Mg^{2+} ion in the N-terminal domain of each β-subunit, site II (Figure 2A). In the $2|F_{o(soak)}| - |F_{o(native)}|$ maps calculated with phases from the native structure, the electron density of the surrounding protein and each molecule of coenzyme A was well-defined.[2] The models were modified

[2] During refinement of the model of dephosphorylated SCS, additional density from Cys 325β became evident, reminiscent of that observed in the native structure of SCS (*4*). This represents anomalous binding of CoA. Only the pantothenate and β-mercaptoethylamine portion of a CoA molecule could be modeled into this density on chain B and refined.

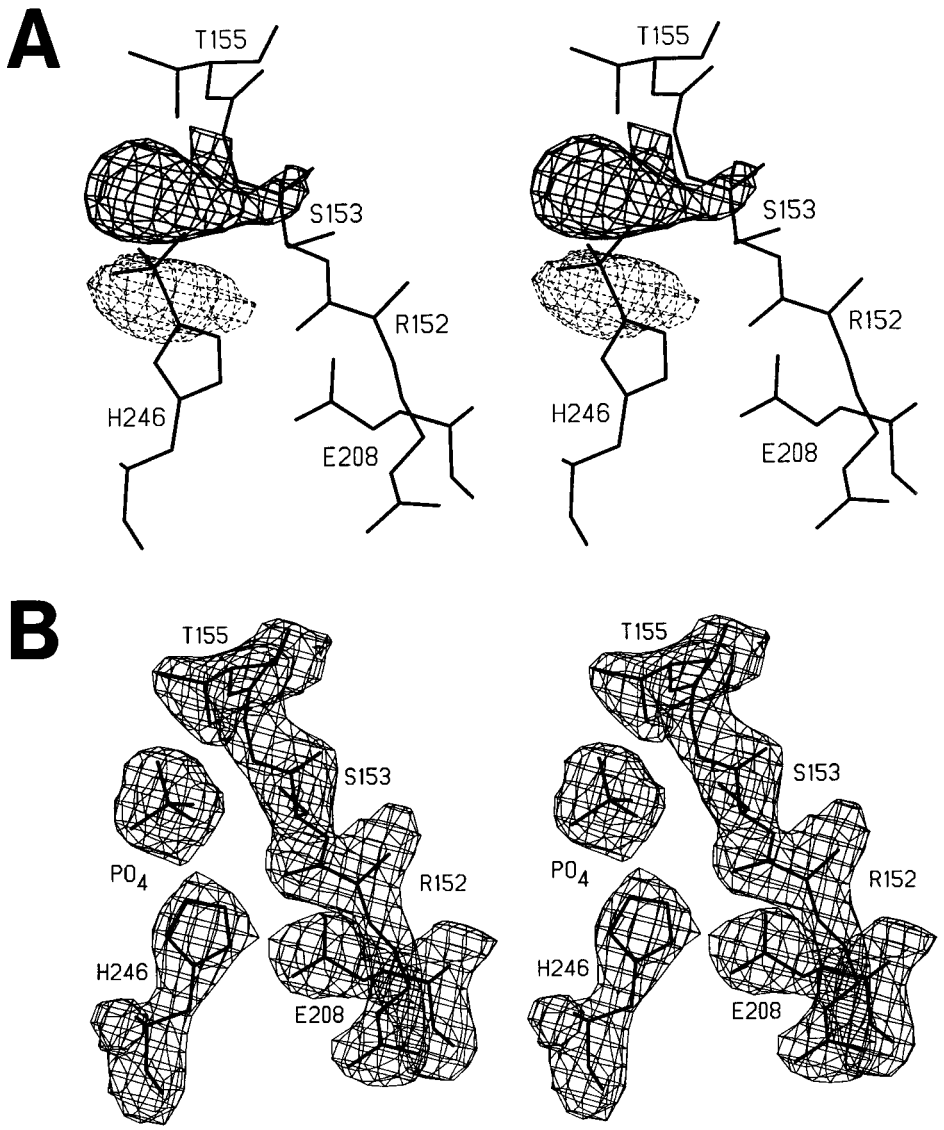

FIGURE 1: Stereo diagrams of electron density in the α-subunit (chain A) in the vicinity of the active site phosphohistidine, His 246α. (A) Initial difference electron density from the $|F_{o(soak)}| - |F_{o(native)}|$ map generated using phases from the native structure of SCS and contoured at -3.3σ (dotted lines) and 3.3σ (solid lines). The bold lines depict amino acid residues of the native model. (B) Electron density from the $2|F_o| - |F_c|$ map generated using the calculated phases from the final model of dephosphorylated SCS, contoured at 1.5σ. The bold lines within the density depict part of the refined model. This figure was drawn using the program TOM (*15*) and the affiliated plotting programs.

to include the observed conformational differences in the protein and the substitution of the β-phosphate of the ADP molecule for the sulfate ion, and then refined. The results of the refinement are outlined in Table 2, and samples of the electron density are shown in Figures 1B and 2B.

In both dephosphorylated models, the hydroxyl group of Ser 153α has rotated to form a hydrogen bond (3 Å) with one oxygen atom of the phosphate ion (Figure 1B). This is the only change common to the two structures in the vicinity of the active site histidine residue, other than the dephosphorylation, that is greater than the lower limit of significance of the experiment. The phosphohistidine loop still interacts with the C-terminal domain of the α-subunit at site I.

The refined model of the ADP molecule bound to SCS is shown in Figure 3A. The ADP molecule lies in the cleft between the two subdomains that constitute the N-terminal domain of the β-subunit. The smaller subdomain includes a four-stranded β-sheet and two α-helices. The larger subdomain has as its core a six-stranded β-sheet. In the structure of the ADP molecule, the adenine ring is oriented anti to the ribose ring with a χ angle (O4*−C1*−N9−C4) of −154° (Figure 3). The conformation of the ADP molecule complexed with the Mg^{2+} ion is depicted in Figure 3B. Residues of the protein that interact with this complex are presented schematically. The adenine ring is sandwiched between the hydrophobic side chains of Val 44β and Leu 212β. The amino group at C6 of the adenine moiety forms hydrogen bonds with one carboxyl oxygen atom of Glu 99β (interatomic distance of 3 Å) and the main chain carbonyl oxygen atom of Ala 100β (3 Å). The N1 atom of the adenine base accepts a hydrogen bond from the main chain amide nitrogen atom of Thr 102β (3 Å). The ribose sugar is held by a hydrogen bond from the 2′-hydroxyl group to one oxygen atom of the carboxyl group of Glu 107β (3 Å). The ϵ-amino group of Lys 46β forms ionic interactions with the α-phosphate group, and the guanidino group of Arg 54β interacts with both the α- and β-phosphate groups. Two of the terminal oxygen atoms of the β-phosphate group form hydrogen bonds

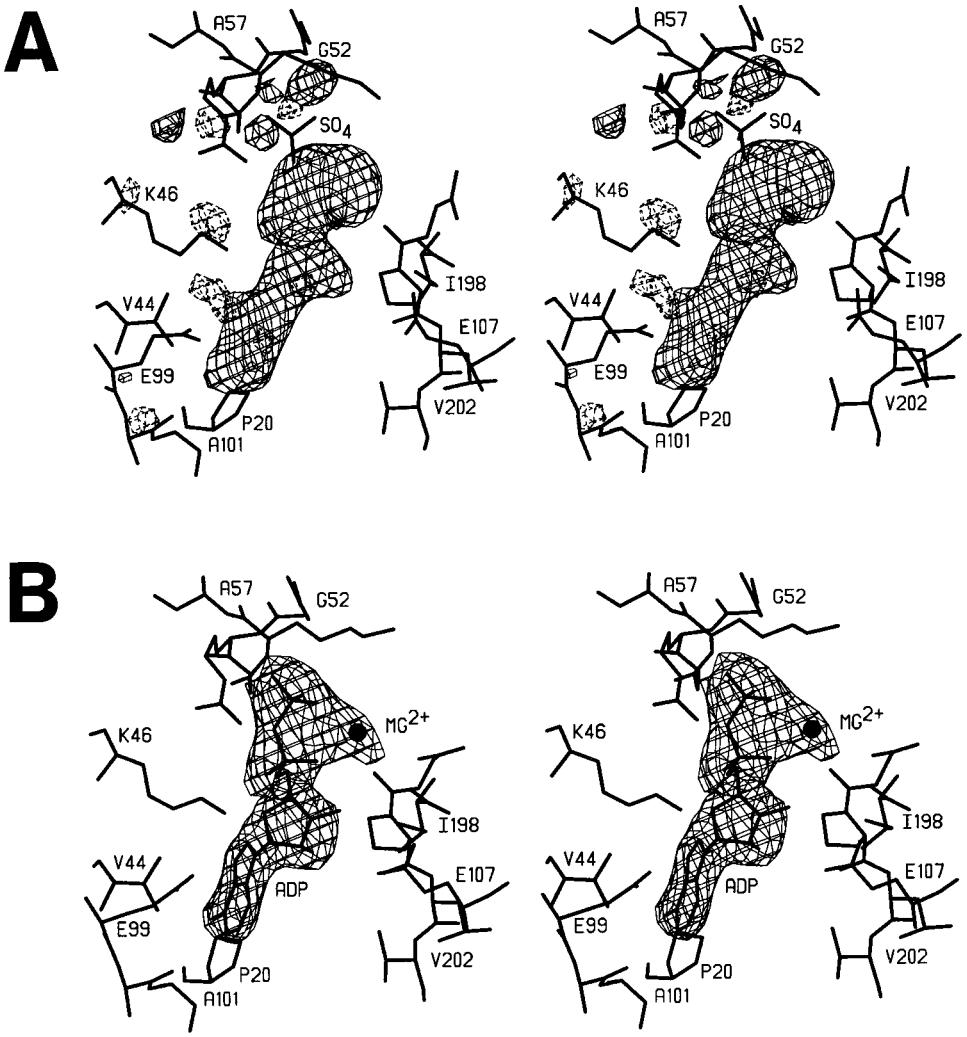

FIGURE 2: Stereo diagrams of electron density in the N-terminal domain of the β-subunit (chain E) from the successful experiment in which crystals of SCS were soaked with ADP and Mg^{2+} ions. (A) Initial difference electron density from the $|F_{o(soak)}| - |F_{o(native)}|$ map generated using phases from the native structure of SCS and contoured at -3.3σ (dotted lines) and 3.3σ (solid lines). The bold lines depict amino acid residues of the native model. (B) Electron density of the ADP$-Mg^{2+}$ complex from the $2|F_o| - |F_c|$ map generated using the phases from the final model of the ADP$-Mg^{2+}$ complex bound to the dephosphorylated SCS, contoured at 1.5σ. The bold lines depict part of the refined model, and the Mg^{2+} ion is shown as a black dot. This figure was drawn using the program TOM (*15*) and the affiliated plotting programs.

Table 2: Refinement Statistics

	first experiment	successful experiment
cell dimensions	$a = b = 98.82$ Å	$a = b = 99.86$ Å
	$c = 404.68$ Å	$c = 407.15$ Å
	$\alpha = \beta = \gamma = 90°$	$\alpha = \beta = \gamma = 90°$
no. of data	45002 (20−2.9 Å)	31753 (20−3.3 Å)
R_{factor}[a] (%)	17.2 (20−2.9 Å)	19.1 (20−3.3 Å)
R_{free}[b] (%)	22.8 (20−2.9 Å)	24.7 (20−3.3 Å)
no. of protein atoms	9892	9892
no. of water molecules	330	0
no. of ligand atoms	133	162
rms deviations from ideal geometry		
bond lengths (Å)	0.016	0.017
bond angles (deg)	1.9	1.9
Ramachandran plot statistics for 1110		
non-proline and non-glycine residues		
no. in most favored regions	1008 (90.8%)	946 (85.2%)
no. in additional allowed regions	100 (9.0%)	158 (14.2%)
no. in generously allowed regions	0 (0%)	4 (0.4%)
no. in dissallowed regions	2 (0.2%)	2 (0.2%)

[a] $R = \Sigma||F_o| - |F_c||/\Sigma|F_o|$. [b] R factor based on data excluded from the refinement (11%).

with the main chain amide nitrogen atoms of residues $53\beta-55\beta$. The Mg^{2+} ion is coordinated by five oxygen atoms, one from each of the α- and β-phosphate groups, one from each of the side chains of Asp 213β and Asn 199β, and the

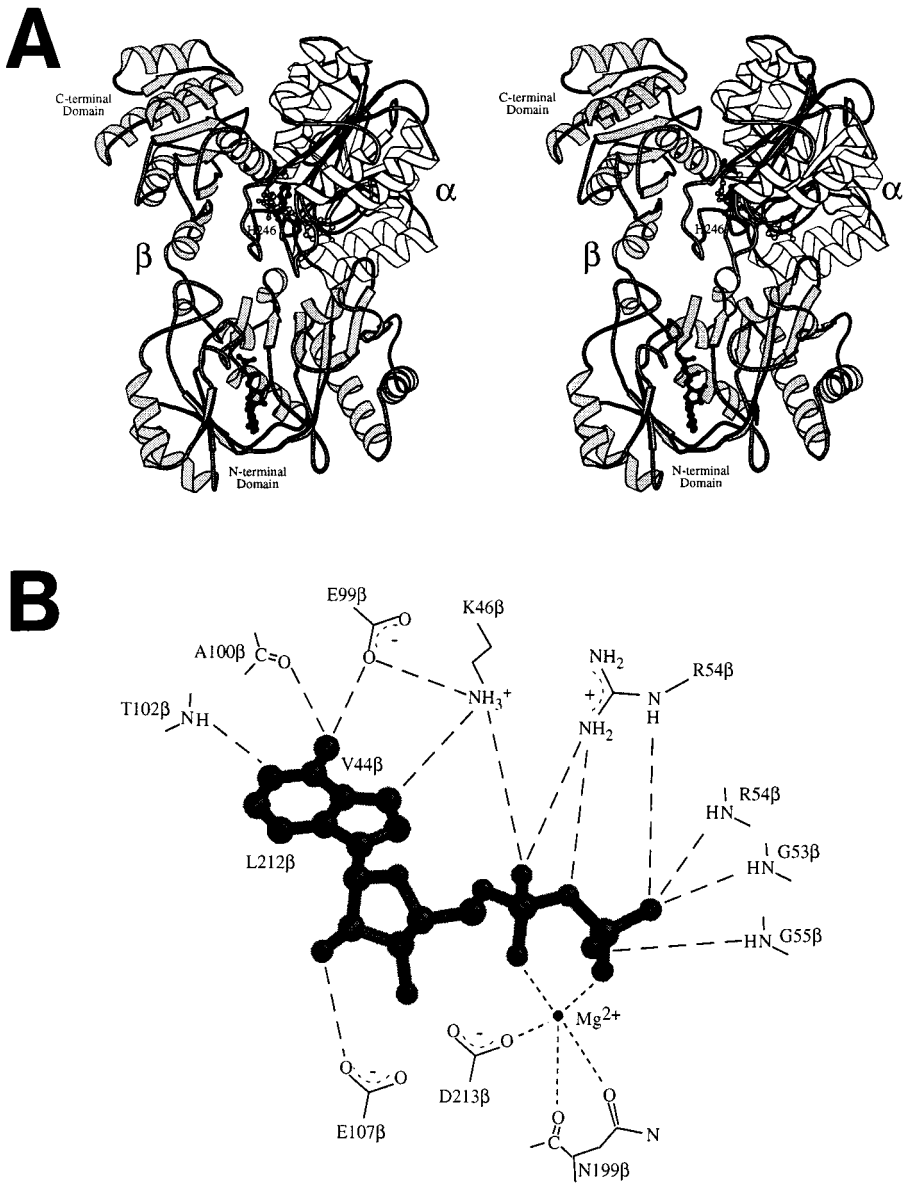

FIGURE 3: Nucleotide binding site of SCS. (A) Stereo ribbon diagram of one $\alpha\beta$-dimer (chains A and B) of *E. coli* SCS with the bound ADP shown as a black ball-and-stick model. The α-subunit is white (except for the side chain of His 246α); the β-subunit is shaded gray, and the molecule of CoA is a white ball-and-stick model. (B) Ball-and-stick model of the ADP−Mg^{2+} complex showing its conformation when bound to SCS. Surrounding residues of SCS that interact with this complex are presented schematically. The lines of long dashes show possible hydrogen bonding interactions. Val 44β and Leu 212β have hydrophobic interactions with the adenine ring. The Mg^{2+} ion is depicted as a large black dot, and is chelated by five ligands as shown by lines of short dashes. This figure was drawn using the program MOLSCRIPT (*35*).

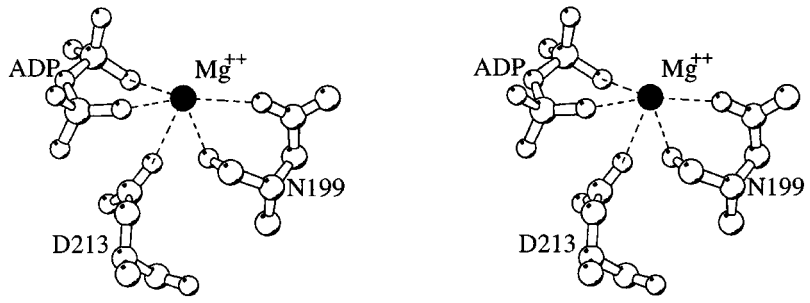

FIGURE 4: Stereo diagram showing the coordination of the Mg^{2+} ion. This figure was drawn using the program MOLSCRIPT (*35*).

fifth from the main chain carbonyl group of Asn 199β (see Figure 4 and the Discussion).

One important difference between the two dephosphorylated structures is located far from the nucleotide binding site. In site I of the SCS model derived from the successful experiment, positive and negative difference electron density required that the model be refitted. The electron density showed that the side chains of Cys 123α and Pro 124α had

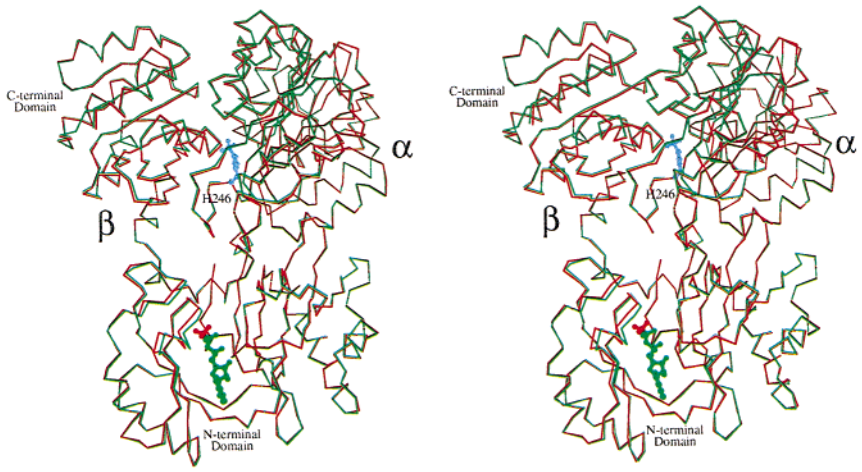

FIGURE 5: Stereo diagram superposing the ADP-bound and native models of an αβ-dimer to show the conformational shift. The ball-and-stick model of the ADP molecule and the corresponding Cα trace are green. The Cα trace of the native enzyme and the ball-and-stick model of the bound sulfate ion are red, while the side chain of His 246α is blue. This figure was drawn using the program MOLSCRIPT (*35*).

"flipped" so that the side chain of the proline residue now packs into the protein interior in the space previously occupied by the sulfhydryl group of the cysteine residue. The cysteine side chain is exposed and forms a disulfide bond with the sulfhydryl group of the CoA molecule. We do not know the relevance of the Cys−Pro flip.

DISCUSSION

The results of the first experiment are germane to the idea that ADP causes dephosphorylation. Since the phosphohistidine can be hydrolyzed nonenzymatically at low pH, it is possible that a drop in pH during the ADP soak was responsible for the dephosphorylation. However, in control experiments it was verified that the pH did not drop below neutrality upon the addition of ADP. Furthermore, as a negative control, trials with nonhydrolyzable nucleotide analogues under identical conditions did not result in dephosphorylation of the enzyme, demonstrating that ADP was responsible for the dephosphorylation. The fact that ADP was not observed bound in the crystal structure can be attributed to low occupancy. At the concentration of ADP used in this experiment, ADP would not be a good competitor for the sulfate and phosphate ions present at high concentrations in the precipitant solution. A sulfate or phosphate ion is seen in both this and the native structure (*7*) bound to the N-terminal domain of the β-subunit. As proved by the structure of the ADP complex with SCS in the successful experiment, the β-phosphate of the nucleotide replaces the sulfate or phosphate ion at this location. Hence, in addition to nonspecific ionic effects, there would be direct competition for the binding site by sulfate and phosphate ions.

On the basis of the results of the first soaking experiment, several modifications were made to the protocols for subsequent experiments culminating in success. The significant changes were lowering as much as possible the concentration of competing ions (e.g., the precipitant sulfate ions), exchanging the buffer (i.e., removing the phosphate ions) so that magnesium ions could be added, and increasing the concentrations of the substrates, ADP and Mg^{2+} ions. The requirement for the excessively high concentration of nucleotide was also demonstrated by an experiment in which the ADP in the final step was replaced with 10 mM β,γ-methyleneadenosine 5′-triphosphate (AMPPCP). This nonhydrolyzable analogue of ATP has a K_i value of 0.38 mM (*25*), more than 1 order of magnitude higher than the K_m for ATP or ADP (*11*, *26*). The enzyme was dephosphorylated by ADP in the preceding steps of the protocol, but the concentration of AMPPCP in the final soak solution was not sufficiently high for it to compete with the sulfate ion and bind in the N-terminal domain of the β-subunit.

Although the binding site for the ADP−Mg^{2+} complex has been identified, full details of the binding cannot be described due to the limited resolution of the data. The soaking experiments caused a deterioration in the crystals. The data to 2.9 Å resolution were used in the analysis of the first experiment, but data to only 3.3 Å resolution were used in the successful experiment. Supposedly, the crystals are less well ordered after the soaking experiments because the enzyme must change conformation to better bind the ADP−Mg^{2+} complex. Figure 5 shows a superposition of the nucleotide-bound structure with the native structure. Parts of the smaller subdomain have moved relative to the rest of the enzyme; however, the helices of this subdomain have not. These helices are constrained because they pack against a second tetramer in the crystals (cf. Figure 7a in ref *7*). However, even these helices can eventually move, since the crystals shattered when left to soak for >48 h. Due to the low resolution of the data, the coordinate errors for the well-ordered atoms in the two models are rather high, estimated as 0.6−0.7 Å (*14*, *27*). In the final refinement of the model from the successful experiment, no water molecules were included. So although it might have been expected that the Mg^{2+} ion would be coordinated octahedrally by six oxygen atoms, in the structure of the complex with SCS the ion is coordinated by five oxygen atoms of the protein (Figure 4). In this model, the sixth position is open to the solution, and presumably, it would be filled by an oxygen atom from a water molecule. Likewise, although we have modeled a phosphate ion next to His 246α, this ion may be a sulfate.

The observed changes in the structure of the protein that accommodate the binding of the ADP−Mg^{2+} complex are relatively small. The inner loop (residues 48β−59β) that

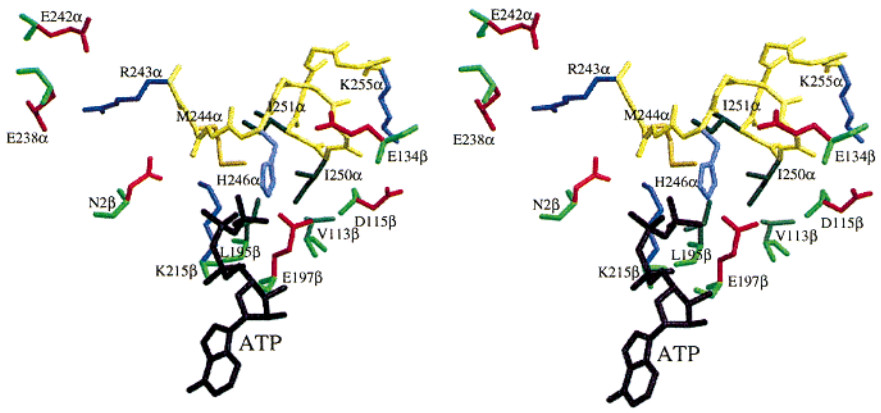

FIGURE 6: Hypothetical model of the His 246α loop at site II depicted in stereoview. The residues of the His 246α loop are shown with yellow backbone atoms. The residues of the β-subunit which may interact with the loop are shown with green backbone atoms. The side chains are colored according to residue type, and the ATP molecule is black. This figure was drawn using the program MOLSCRIPT (*35*).

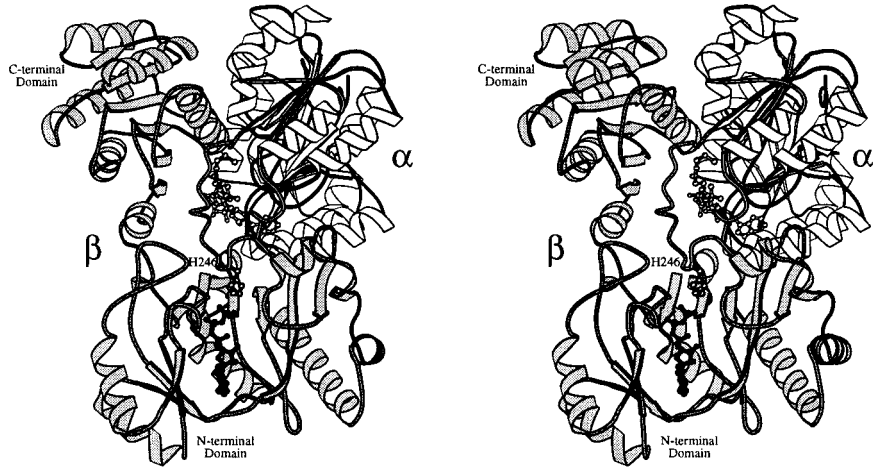

FIGURE 7: Stereo ribbon diagram of an $\alpha\beta$-dimer of SCS with the hypothetical model of the His 246α loop at site II. The ATP molecule is represented by a black ball-and-stick model. This figure was drawn using the program MOLSCRIPT (*35*).

complexes the free sulfate ion in the native structure is shifted in toward the cleft to bind the β-phosphate of ADP. The neighboring loop (residues 82β−90β) also shifts so that its interactions with the inner loop can be maintained (Figure 5). The side chain carboxylate group of Asp 213β provides one ligand for the Mg^{2+} ion. As a result, the hydrogen bond observed in the native structure between one carboxylate oxygen atom and the nitrogen atom of Gly 214β must be broken. The plane of the peptide bond between Asp 213β and Gly 214β is rotated in the complex relative to that in the native structure, and the carbonyl oxygen atom adopts a position more favorable for accepting a hydrogen bond (3 Å) from the amide nitrogen atom of Asn 199β. The use of the side chain oxygen atom, Oδ1, of Asn 199β to coordinate the Mg^{2+} ion disrupts hydrogen bonding interactions in the native structure between the side chain amido group of Asn 199β and both the amide nitrogen atom of Gly 130β and the carbonyl oxygen atom of Val 131β. Residues Gly 130β and Val 131β are part of one tryptic peptide that was found labeled by 8-N_3-ATP (*8*). The loop containing these residues is structurally analogous to the "lid" over the nucleotide in DD-ligase (*28*) and glutathione synthetase (*29*), two other enzymes possessing the ATP-grasp fold (*6*). Primarily due to the absence of a lid, 47% of the ADP molecule when bound by SCS is accessible to solvent, in contrast to 2% when bound by DD-ligase.[3] Surprisingly, there is very little change in the position of Glu 107β. By analogy to DD-ligase, the carboxylate group of this side chain was expected to form hydrogen bonds with the 2′- and 3′-hydroxyl groups of the ribose moiety (*7*). Instead, only one oxygen atom of the carboxylate group interacts with the 2′-hydroxyl group, and this is with a long distance of >3 Å. This is similar to the binding in synapsin I (*34*).

The ADP−Mg^{2+} complex is bound by residues of both subdomains of the N-terminal domain of the β-subunit with only these small changes. This contrasts with our earlier hypothesis that the two subdomains would close so that each would superpose with its counterpart of DD-ligase. Instead, when the superposition of the two structures is based on the ADP molecules,[4] the β-sheets of the smaller subdomain superpose quite well, while those of the larger subdomains do not. Instead, the β-strands of this subdomain of SCS are in the same plane as those of DD-ligase, but there is an angle

[3] The surface areas of the molecules accessible to solvent were calculated using the program MS (*30*).

[4] The superposition was carried out using the program SUPPOS from the BIOMOL package.

of about 20° between the directions of the strands. It may be that the orientation of one subdomain with respect to the other need not be identical among structures possessing the ATP-grasp fold. However, one may wonder if SCS is truly in the conformation it would adopt when binding the ADP−Mg^{2+} complex in solution.

The conformation of the inner loop that binds the β-phosphate of ADP (residues 53β−55β) is different from that observed in other proteins possessing the ATP-grasp fold. Although Thoden et al. (*31*) postulated that the type III′ reverse turn seen to bind the nucleotide in carbamoyl phosphate synthetase (*31*), glutathione synthetase (*29*), and DD-ligase (*28*) may be common to all proteins of this family, SCS and pyruvate phosphate dikinase (*32*) are the current exceptions. Because pyruvate phosphate dikinase transfers the γ,β-pyrophosphate group of ATP as a single unit, the conformation of this loop would be expected to be different. In SCS, the side chain of Arg 54β interacts with the phosphates of ADP, replacing Lys 97 of DD-ligase (*28*), Lys 125 of glutathione synthetase (*29*), or Arg 675 of carbamoyl phosphate synthetase (*31*), residues that are not part of the reverse turn. The conformation of Gly 53β-Arg 54β-Gly 55β in SCS is reminiscent of the conformation of three residues of the phosphate-binding loop of G proteins, e.g., Gly 15-Lys 16-Ser 17 of H-ras p21 (*33*). Each forms hydrogen bonds with the β-phosphate of the nucleotide; however, if the three residues in the two proteins are superposed, the nucleotides are oriented in opposite directions so that the α-phosphate of ADP bound to SCS superposes with the γ-phosphate of the nucleotide bound to H-ras p21.

These are the first structures of dephosphorylated SCS that have been observed. In the native, phosphorylated structure, there was a water molecule bound to the phosphoryl group of chain A at site I (*7*). It was postulated that this water molecule was in the position that the oxygen atom of succinate might adopt prior to the transfer of the phosphoryl group from the phosphohistidine. This interpretation is supported by the dephosphorylated structures wherein one of the oxygen atoms of the phosphate ion (O4) adopts this position. Interactions between the protein and the other three oxygen atoms are similar in the phosphorylated and dephosphorylated structures, with the exception of the previously mentioned change in χ_1 of Ser 153α. This change allows the Oγ atom of Ser 153α to interact with oxygen atom O1 of the phosphate ion. The environments of the three oxygen atoms covalently attached to the phosphorus atom could be maintained as the phosphoryl group is transferred from the phosphohistidine to form succinyl phosphate and released as a phosphate ion at site I. These three oxygen atoms would be in the equatorial plane, while the nitrogen atom of the imidazole ring and the fourth oxygen atom would adopt the axial positions about the phosphorus atom in the trigonal bipyramidal transition state.

Since the nucleotide binds in the N-terminal domain of the β-subunit (site II) and the phosphorylated His 246α is observed ∼35 Å away at site I, we postulated that the loop containing this histidine residue must "swing" between the two sites during catalysis (*7*). Now, if one presumes that the γ-phosphate group of ATP has the same orientation relative to the imidazole ring as the phosphate ion in the dephosphorylated structure, the O4 atom of the phosphate ion can be positioned on one of the terminal oxygen atoms of ADP to model ATP.[5] The terminal oxygen atom chosen as the β,γ-bridging atom of ATP was the one that allowed the modeled γ-phosphate group to coordinate the Mg^{2+} ion. This choice is consistent with the structures of ATP analogues bound to carbamoyl phosphate synthetase (*31*) and synapsin I (*34*). The positioning of the phosphate ion also orients a possible conformation of the His 246α loop prior to phosphorylation at site II. For this modeling, the loop was detached from the rest of the α-subunit by breaking the Cα−C bond of residue 241α and the N−Cα bond of residue 253α, and the loop was rotated about the position of the Cα atom of residue 253α so that the angle at the β,γ-bridging oxygen atom of ATP was approximately 109°. The movement orients the imidazole ring so that Nδ1 is directed toward Glu 197β. We had predicted earlier that Glu 197β would form a hydrogen bond with Nδ1 of the imidazole ring when His 246α is bound at site II (*7*). To improve the model, the torsion angles along the polypeptide chain were adjusted so that the hydrophobic side chains of residues Met 244α, Ile 250α, and Ile 251α interacted with Leu 195β and Val 113β, and so that the termini of the loop were directed toward residues 240α and 254α. The loop was reattached, and the geometry of residues 239α−242α and residues 251α−256α was regularized. This model of the His 246α loop in site II is depicted in Figure 6. It must be emphasized that this conformation of the loop is purely hypothetical, based only on the knowledge that His 246α must move from where it is seen in the structure to where the nucleotide binds. Lending credence to this model is the fact that residues of the β-subunit that would interact with the active site loop are conserved in known sequences of SCS. For example, residues equivalent to 113β and 195β are usually hydrophobes. Residue 115β is usually Asp, but can be Glu; residues 134β and 197β are Glu, and residue 215β is predominantly Lys, but can be Arg. This model in the complete αβ-dimer is shown in Figure 7. A comparison of Figure 7 with Figure 3A shows that there is space for the loop to move unencumbered by any other part of SCS. This working model of the loop interacting at site II will be useful in suggesting further experiments that will extend our understanding of the mechanism of the phosphorylation of His 246α by nucleotide.

[5] The modeling was done using the program TOM *(15)*.

ACKNOWLEDGMENT

We acknowledge Edward Brownie for his technical expertise in producing and purifying the protein, Noriyoshi Sakabe, Atsushi Nakagawa, and Nobuhisa Watanabe for provision of beam time and assistance at the Photon Factory, and Chris Rochet for help with the data collection.

REFERENCES

1. Bridger, W. A. (1974) *The Enzymes (3rd Ed.) 10*, 581−606.
2. Nishimura, J. S. (1986) *Adv. Enzymol. 58*, 141−172.
3. Bailey, D. L., Fraser, M. E., Bridger, W. A., James, M. N. G., and Wolodko, W. T. (1999) *J. Mol. Biol. 285*, 1655−1666.
4. Wolodko, W. T., Fraser, M. E., James, M. N. G., and Bridger, W. A. (1994) *J. Biol. Chem. 269*, 10883−10890.
5. Johnson, J. D., Muhonen, W. W., and Lambeth, D. O. (1998) *J. Biol. Chem. 273*, 27573−27579.

6. Murzin, A. G. (1996) *Curr. Opin. Struct. Biol. 6*, 386−394.
7. Fraser, M. E., James, M. N. G., Bridger, W. A., and Wolodko, W. T. (1999) *J. Mol. Biol. 285*, 1633−1653.
8. Joyce, M. A., Fraser, M. E., Brownie, E. R., James, M. N. G., Bridger, W. A., and Wolodko, W. T. (1999) *Biochemistry 38*, 7273−7283.
9. Wolodko, W. T., Kay, C. M., and Bridger, W. A. (1986) *Biochemistry 25*, 5420−5425.
10. Wolodko, W. T., James, M. N. G., and Bridger, W. A. (1984) *J. Biol. Chem. 259*, 5316−5320.
11. Moffet, F. J., Wang, T., and Bridger, W. A. (1972) *J. Biol. Chem. 247*, 8139−8144.
12. Ray, W. J., Jr., Bolin, J. T., Puvathingal, J. M., Minor, W., Liu, Y., and Muchmore, S. W. (1991) *Biochemistry 30*, 6866−6875.
13. Sakabe, N. (1991) *Nucl. Instrum. Methods Phys. Res. A303*, 448−463.
14. Read, R. J. (1986) *Acta Crystallogr. A42*, 140−149.
15. Jones, T. A. (1985) *Methods Enzymol. 115*, 157−171.
16. Engh, R. A., and Huber, R. (1991) *Acta Crystallogr. A47*, 392−400.
17. Brunger, A. T. (1992) *Nature 355*, 472−474.
18. Kleywegt, G. J., and Brunger, A. T. (1996) *Structure 4*, 897−904.
19. Pannu, N. S., and Read, R. J. (1996) *Acta Crystallogr. A52*, 659−668.
20. Adams, P. D., Pannu, N. S., Read, R. J., and Brunger, A. T. (1997) *Proc. Natl. Acad. Sci. U.S.A. 94*, 5018−5023.
21. Brunger, A. T., Adams, P. D., and Rice, L. M. (1997) *Structure 5*, 325−336.
22. Brunger, A. T., Adams, P. D., Clore, G. M., Delano, W. L., Gros, P., Grosse-Kunstleve, R. W., Jiang, J.-S., Kuszewski, J., Jilges, N., Pannu, N. S., Read, R. J., Rice, L. M., Simonson, T., and Warren, G. L. (1998) *Acta Crystallogr. D54*, 905−921.
23. Laskowski, R. A., MacArthur, M. W., Moss, D. S., and Thornton, J. M. (1993) *J. Appl. Crystallogr. 26*, 283−291.
24. Hooft, R. W. W., Vriend, G., Sander, C., and Abola, E. E. (1996) *Nature 381*, 272.
25. Vogel, H. J., and Bridger, W. A. (1982) *J. Biol. Chem. 257*, 4834−4842.
26. Moffet, F. J., and Bridger, W. A. (1970) *J. Biol. Chem. 245*, 2758−2762.
27. Luzzati, V. (1952) *Acta Crystallogr. 5*, 802−810.
28. Fan, C., Moews, P. C., Walsh, C. T., and Knox, J. R. (1994) *Science 266*, 439−443.
29. Hara, T., Kato, H., Katsube, Y., and Oda, J. (1996) *Biochemistry 35*, 11967−11974.
30. Connolly, M. L. (1983) *Science 221*, 709−713.
31. Thoden, J. B., Wesenberg, G., Raushel, F. M., and Holden, H. M. (1999) *Biochemistry 38*, 2347−2357.
32. McGuire, M., Huang, K., Kapadia, G., Herzberg, O., and Dunaway-Mariano, D. (1998) *Biochemistry 37*, 13463−13474.
33. Pai, E. F., Krengel, U., Petsko, G. A., Goody, R. S., and Kabsch, W. (1990) *EMBO J. 9*, 2351−2359.
34. Esser, L., Wang, C., Hosaka, M., Smagula, C. S., Sudhof, T. C., and Deisenhofer, J. (1998) *EMBO J. 17*, 977−984.
35. Kraulis, P. J. (1991) *J. Appl. Crystallogr. 24*, 946−950.

BI991696F